MDPI

Article

Simulation Analysis of Fuel Economy of the GDI Engine with a Miller Cycle and EGR Based on GT-Power

Shengli Wei *[ID]**, Zhicheng Zhang, Xuan Li, Chengcheng Wu and Fan Yang**

School of Automotive and Traffic Engineering, Jiangsu University, Zhenjiang 212013, China; zzc13581377801@163.com (Z.Z.); zjldlb0810@163.com (X.L.); work_wu1995@163.com (C.W.); 2211904057@stmail.ujs.edu.cn (F.Y.)
* Correspondence: weishengli@ujs.edu.cn

Abstract: A one-dimensional (1D) simulation calculation model was created using GT-Power software to investigate the effect of an exhaust gas recirculation (EGR) in concert with the Miller cycle on engine fuel economy and using a 1.5 T gasoline direct injection (GDI) engine as the source engine. The engine was tested under partial loading, full loading, and declared working conditions. The results show that under partial load, the Miller cycle could improve engine fuel economy by reducing pumping losses. In the low-speed 1000 r/min full load region, the Miller cycle had a significant effect on increasing the engine fuel economy. When the Miller intensity was −29 °CA, the fuel consumption decreased by a maximum of 10.5%. At medium speeds, 2000 r/min to 3600 r/min, the Miller cycle did not improve fuel economy significantly. For the Miller cycle with late intake valve closure (LIVC), when the EGR rate was about 7%, the fuel consumption was reduced by about 1.3% compared with the original engine at the same EGR rate. When opposed to the original engine without EGR, the fuel consumption was lowered by approximately 3.2 percent.

Keywords: GDI engine; Miller cycle; EGR; simulation; fuel economy

1. Introduction

Increasingly stringent energy conservation and emission regulations are driving continuous innovation in the field of engine technology and innovations. In order to improve engine fuel economy, researchers mainly start from the combustion process and the mechanical part. Hunicz et al. [1] studied the combustion stability of SACL (spark-assisted compression ignition) in an attempt to improve thermal efficiency and reduce NOx emissions by studying the SACL/HCCL (homogeneous charge compression ignition) transition. By analyzing the shape of the piston ring, Wróblewski et al. [2,3] tried to improve the mechanical efficiency and achieve the purpose of increasing the thermal efficiency. In recent years, the Miller cycle and EGR technology also have become research hotspots due to their inhibitory effect on knocking and improved economics [4–7]. Engine fuel consumption can be decreased using both the Miller cycle and EGR technology. The Miller cycle reduces the effective compression ratio of a piston through early or late intake valve closure (EIVC or LIVC) to achieve an over-expanded cycle, thereby reducing fuel consumption. EGR technology introduces exhaust gas into a cylinder to participate in combustion again, reducing throttle loss and heat transfer loss, thereby improving engine fuel economy.

Most work done on this subject [8–17] has adopted different control strategies. Mazda created the first mass-produced Miller cycle engine, which became an automotive unit in 1993 [18], with up to a 15% decrease in brake-specific fuel consumption. Li et al. [19] investigated the impacts of the Miller cycle, which were applied to a GDI engine with a geometric compression ratio (CR) of 12.0 in an experimental setting. The results revealed that using a high load operation with LIVC increased fuel economy by 4.7 percent. The LIVC and EIVC both reduced fuel consumption by 6.8% and 7.4%, respectively, when operating

at low loads. Cleary et al. [20] explored the potential for partial load fuel consumption using EIVC variable valve actuated single-cylinder engines that operated without throttling. They showed that by optimizing the intake lift for duration and timing while keeping traditional exhaust valve events, they could reduce fuel consumption by approximately 7%. Wan et al. [21] analyzed the potential benefits of the Miller cycle for a high CR SI engine, concluding that EIVC with a low valve lift should be used for a partial load to increase thermal efficiency. Miklanek et al. [10] studied the Miller and Otto cycles, two common thermodynamic cycles. The results indicated that, compared with the Otto cycle, fuel economy was significantly improved, especially because of the application of the Miller cycle. It was very effective to improve the fuel economy by introducing an EGR system that increases the external cooling function [22,23]. Fontana et al. [24] studied a naturally aspirated spark-ignition gasoline engine and found that under a high load, the EGR could improve the advance of the ignition advance angle without knocking and optimize the combustion phase to increase the fuel economy of the engine. Under a low load, the thermal efficiency could be improved by reducing the pumping loss. Zhang et al. [25] combined tumble flow, and Liu et al. [26] and Song et al. [27] combined changes in the compression ratios to obtain the reduced fuel consumption results. Wang et al. [28] found that under low speed and heavy load operations, the use of the Miller cycle worsened soot emissions, while EGR technology reduced engine fuel consumption by 8.6% and alleviated soot emissions.

There are now a few studies on the effects of the Miller cycle and EGR on a GDI engine using the WoschniGT heat transfer model and the EngCylCombSIWiebe combustion model. Because GT-Power software can provide effective solutions for the selection and matching of various engine components, it can also calculate an engine's power, torque, fuel consumption, and emissions performance, providing engine development and transformation reference [29,30].

In this study, the Miller cycle effects of EIVC and LIVC on the fuel economy of a GDI engine are simulated with the GT-Power model and compared at low, medium, and high speeds. The effects of different intensity Miller cycles combined with EGR on engine performance are discussed.

2. Methodology

2.1. Computational Fluid Dynamics Model

The object of this paper was a 1.5 T gasoline engine, which was a four-stroke turbocharged GDI engine. Table 1 lists the engine's main parameters. In this study, a 1D simulation model of the engine was created using GT-Power software based on the structural parameters and technical specifications of each component of the gasoline engine, as shown in Figure 1. The software could simulate the intake, compression, power, exhaust, heat transfer, and gas flow in the pipeline of an internal combustion engine, and analyze and optimize of the key parameters. The model was mainly composed of the intake pipe, throttle, intake valve and intake manifold, injector, cylinder, crankcase, exhaust valve, exhaust manifold, turbocharger, and exhaust tail pipe.

Table 1. The main parameters of the engine.

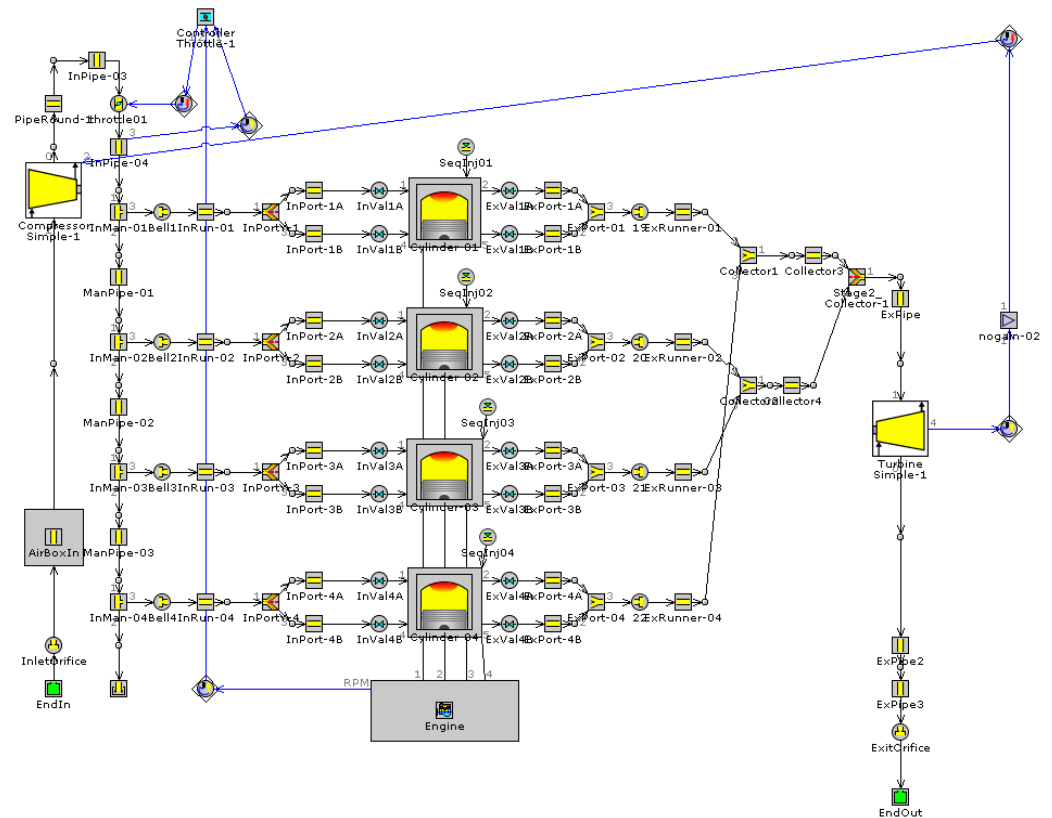| Project	Value
Layout form	In-line four-cylinder
Engine type	Turbocharger + GDI + air intake cooling
Bore diameter/mm × stroke/mm	74 × 86.6
Connecting rod length/mm	126.8
Compression ratio	10.5
Nozzle hole number	6
Intake manifold volume/L	0.9
Maximum in-cylinder pressure/MPa	10
Maximum power/speed kW/(r/min)	122/5450
Maximum torque/speed N·m/(r/min)	256/2250

Figure 1. Simulation model of the engine.

Since the gasoline engine used quantity regulation to manage the engine load, the intake volume of the intake pipe was adjusted by throttle, thereby achieving the regulation of the engine load. The air intake volume of the first section of the pipe behind the throttle was within the error range of 2% with that of the original engine by setting the opening of the throttle valve. In GT-Power software, the intake and exhaust pipes were set as straight pipes with a circular cross-section, and the initial values such as friction coefficient, heat transfer coefficient, and pressure loss coefficient were set according to the actual conditions of the engine's intake and exhaust pipes. In addition, the engine had turbocharging and intercooling, so the second section of pipeline after the compressor, InPipe-03, was set as the intercooler, and the wall temperature was set to the temperature after intercooling.

The GT-Power software provided two turbocharger models. Considering the actual conditions of the research content in this study, a simple turbocharger model was selected in order to transfer the work that is actually generated by the turbine to the compressor. The efficiency that was set by the compressor was the efficiency estimated using the experimental value. The nozzle diameter of the turbine was variable, and the pressure was controlled by adjusting the nozzle diameter.

The intake and exhaust valves were key components for controlling the gas exchange between the cylinder and the outside, and they were important components for realizing the Miller cycle. The valve opening time and valve lift curve were set in the valve train in order to achieve the automatic adjustment of the valve movement law, which was of great significance for the subsequent realization of the Miller cycle through variable valves, which could greatly reduce the calculation cycle and data analysis workload.

The injector module automatically calculated the injection quantity based on the air intake volume and air–fuel ratio. For the injection component, the relevant fluid setting template was called in the injector model and the relevant parameters in the template were filled in according to the gasoline-related indicators. The injection substance used for simulation was gasoline.

The cylinder was the core component of the entire model. The most complicated combustion and heat transfer part of the entire model was also the cylinder module. Therefore, the setting of the cylinder module was very important. The initial state and wall temperature, as the starting state and combustion boundary of the entire combustion process, had a certain influence on the convergence speed and accuracy of the simulation. In addition, the selection of the heat transfer model and combustion model had great influence on the entire simulation calculation. Based on the actual simulation requirements, the WoschniGT heat transfer model and the Wiebe combustion model were selected to simplify the in-cylinder motion and combustion processes of the engine. Finally, the engine speed, main geometric structure size, ignition sequence, and other aspects were placed in the corresponding position of the engine module, and the entire one-dimensional thermodynamic model was completed.

2.2. Validation of Computational Fluid Dynamics Model

In order to achieve accurate simulation of the working process of the engine, the seven common operating conditions shown in Table 2 were selected to calibrate the relevant parameters of the combustion and turbocharger.

Table 2. The main parameters of the selected operating conditions.

Operating Conditions	Speed /(r·min^{-1})	Load	Torque /(N·m)	Power /(kW)	Fuel Consumption /(g·(kW·h)$^{-1}$)
1	1000	50%	71.3	7.47	258.99
2	1000	100%	151.9	15.91	291.31
3	2000	50%	118.3	24.78	235.01
4	2000	100%	246	51.51	289.41
5	3600	50%	130.2	49.09	243.32
6	3600	100%	249.6	94.11	317.92
7	5600	100%	202.9	118.98	371.43

In order to eliminate the interaction between the turbocharger and the cylinder, the combustion parameters were calibrated using a model without a turbocharger. Figure 2 depicts the comparison of numerically and experimentally determined air intake volume and in-cylinder pressure values. The simulation values were in good agreement with the experimental values, and the calibrated combustion model has a particular responsiveness to the original engine's real combustion process, as shown in the figure.
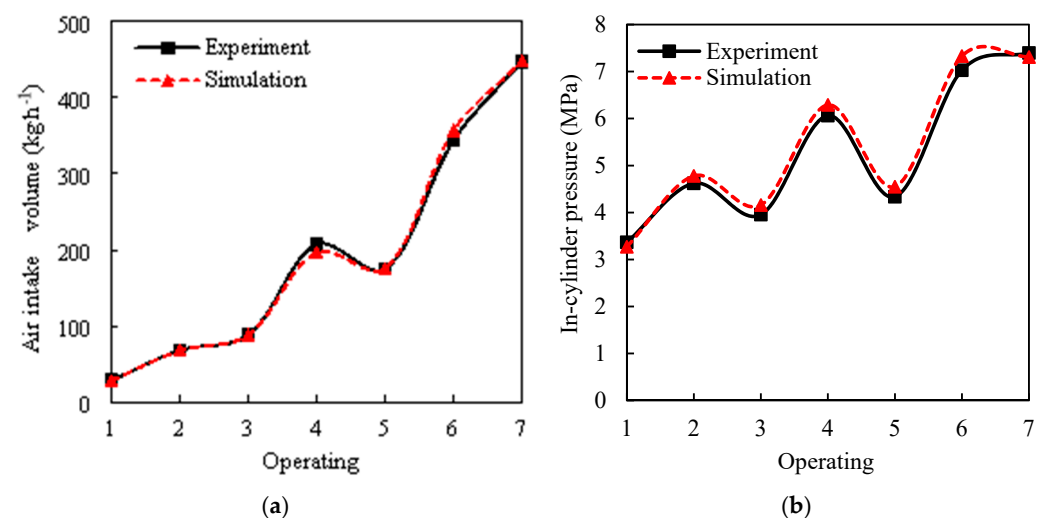

(**a**)

(**b**)

Figure 2. Comparison of the experimental and simulation values under different operating conditions: (**a**) determined air intake volume, (**b**) in-cylinder pressure values.

3. Results and Discussion

After the calibration of the combustion model was completed, the model with the turbocharger was calibrated. As Figure 3 shows, for the seven common operating conditions of the GDI engine, the main performance parameters of the engine at the test point coincided well with those of the original engine. The difference between the experimental and simulated values was less than 5%. As a consequence, the calculation models met the calculation criteria, the engineering study had some value, and the calculation result was reliable.
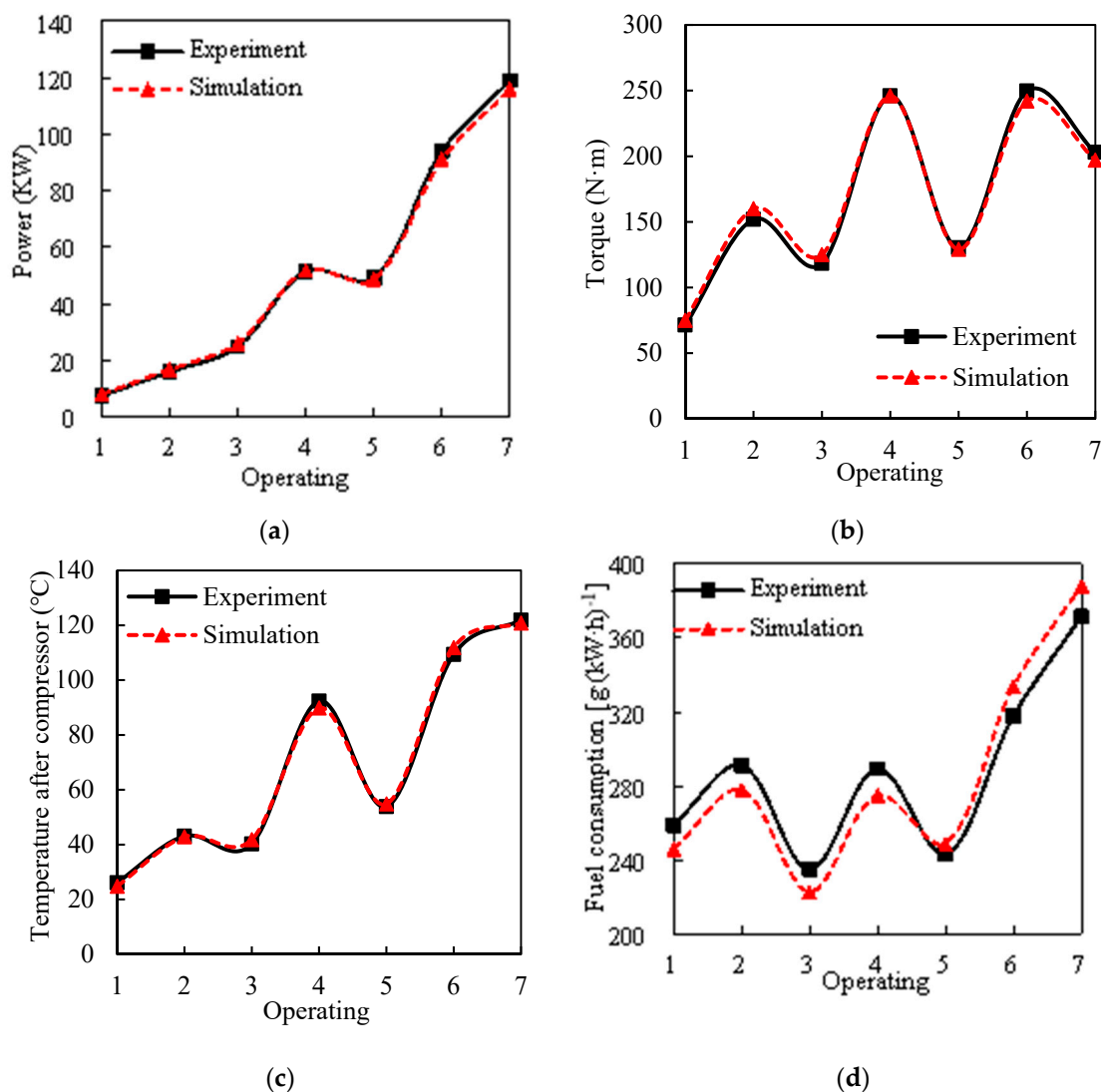

(**a**)

(**b**)

(**c**)

(**d**)

Figure 3. Comparison of the experimental and simulation values under different operating conditions: (**a**) power, (**b**)torque, (**c**) temperature after compressor, (**d**) Fuel consumption.

The duration of the intake valve opening and the maximum intake valve lift are changed to realize the Miller cycle [31]. By increasing the valve closing angle and matching the opening time and duration of the intake valve of the original engine, the adjustment coefficient of the opening duration of the intake valve was calculated from Equation (1). Meanwhile, to meet the requirements of the dynamics, corresponding adjustments should also be made for the intake valve lift; when the adjustment coefficient of the valve lift is the square of the adjustment coefficient of the valve opening duration, the dynamic demand can be met (Equation (2)):

$$X = (a - b)/d \tag{1}$$

$$Y = X^2 \tag{2}$$

where *a* is the valve closing angle, *b* is the opening time of the intake valve, d is the duration of the intake valve, *X* is the adjustment coefficient of the opening duration of the intake valve, and *Y* is the adjustment coefficient of the valve lift.

In this study, the difference between the actual IVC and the original IVC moment was defined as the Miller intensity. When the Miller intensity was 0 °CA, it represented the original engine. Table 3 shows the nine Miller cycle schemes that were designed in this study. A negative Miller intensity represented EIVC, while a positive Miller intensity represented LIVC. As shown in Figure 4, ten groups of the curve of the valve lift were designed, including the original engine. The design curve of valve lift was used as the input value, and the throttle opening was adjusted to ensure that the air intake volume was the same, that is, that the load remained the same. The change of the engine economy under different Miller strengths was studied.

Table 3. Miller cycle schemes.

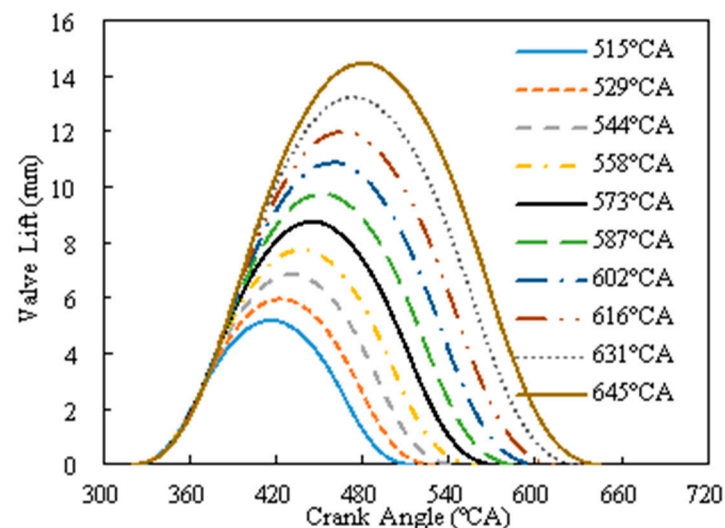| Miller intensity (°C\A)	−58	−44	−29	−15	0	14	29	43	58	72
Closing time of the intake valve (°CA)	515	529	544	558	573	587	602	616	631	645

Figure 4. The curves of the valve lift.

There were two main forms of influence of Miller cycle on engine performance for the gasoline engine that control engine load by quantity regulation. On the one hand, under partial load conditions, the use of Miller cycle will reduce the engine charging efficiency and affect the engine's power performance. In order to ensure that the power performance remained unchanged, the method of increasing the throttle opening was adopted to keep the air intake volume constant. The benefit was that it reduces air intake throttling losses, thereby reducing pumping losses and further improving fuel economy. On the other hand, for full load conditions, because the valve was fully open at this time, if the Miller cycle was adopted, it inevitably brings about a drop in the charging efficiency and the mass of air intake, which reduces the engine power and torque. In order to ensure constant power performance, it was necessary to adjust the turbocharger to improve the intake pressure, ensure the intake volume, achieve high density and low temperature combustion, improve thermal efficiency, and reduce the emission of pollutants and the risk of knocking.

The fuel consumption chart for the universal characteristic of the engine studied is shown in Figure 5. Based on the analysis above and the common operating conditions of the engine, two sets of operating conditions were finally selected as the research objects.

The first group was a 50% load condition with common speed from 1000 to 3600 r/min, implemented to study the improvement of pumping loss and fuel economy optimization by the Miller cycle. The second group was the common to full load operating conditions and the engine calibration operating conditions from 1000 to 5600 r/min. It was used to study the improvement of thermal efficiency of the Miller cycle and the demand of the turbocharger under full load operating conditions.
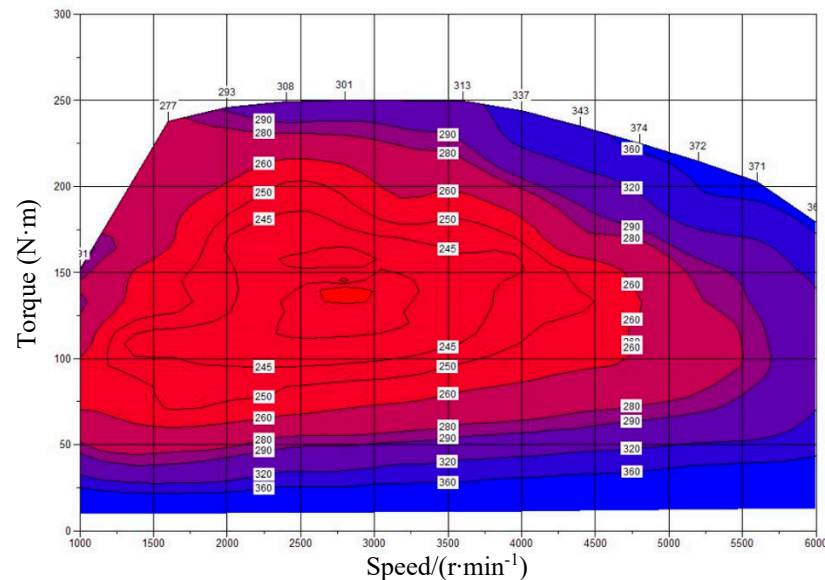

Figure 5. Engine fuel consumption chart for the universal characteristic.

3.1. Effect of the Miller Cycle on the Fuel Economy at Partial-Loading Operating Conditions

Figure 6 depicts the influence of the intake valve closing time on fuel consumption at various speeds when operating at 50% load. With the time of the intake valve closing, the fuel consumption showed a tendency to be low for the two ends and high for the middle. As the Miller intensity increased, the fuel consumption decreased, because as the throttle opening became larger, the pumping loss was reduced. When the Miller intensity was 43 °CA, the fuel consumption of the engine was reduced by 0.4%, 0.5%, and 1.2% compared to the original engine at 50% load conditions at 1000, 2000, and 3600 r/min. When the Miller strength was −44 °CA, the fuel consumption of the engine was reduced by 1.2%, 1.3%, and 2.4%, respectively. When the Miller intensity reached a maximum of 72 °CA, the fuel consumption was lowered by 2.1%, 1.8%, and 2.4%.
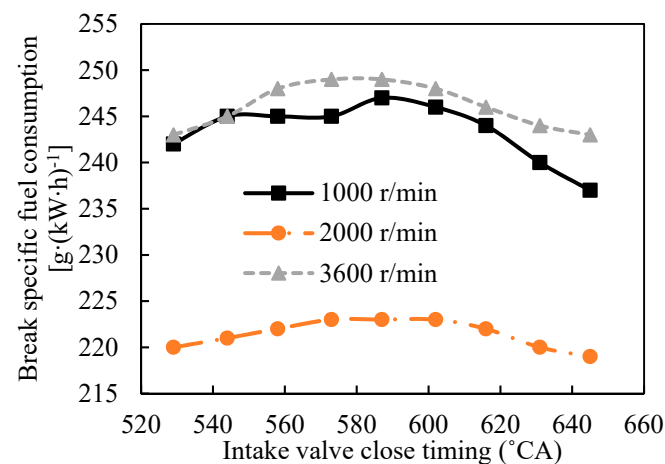

Figure 6. Effect of the intake valve closing timing on the fuel consumption at different speeds under 50% load.

In order to further analyze the reasons for the improved fuel economy compared to the original engine after adopting the Miller cycle, Figures 7 and 8, respectively, show the influence of the intake valve closing time on the throttle opening and pumping loss under different speeds and 50% load conditions.
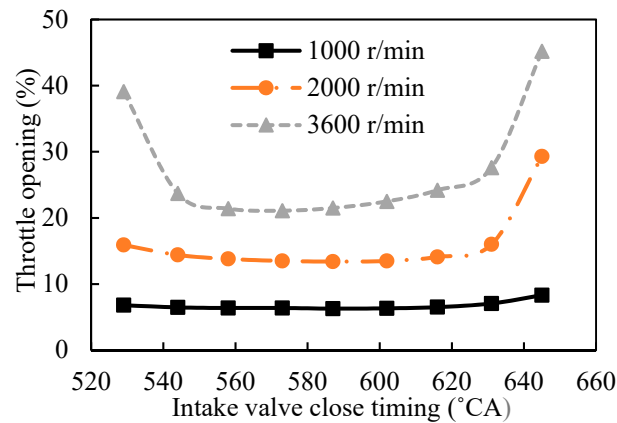

Figure 7. Effect of intake valve close timing on throttle opening at different speeds under 50% load.
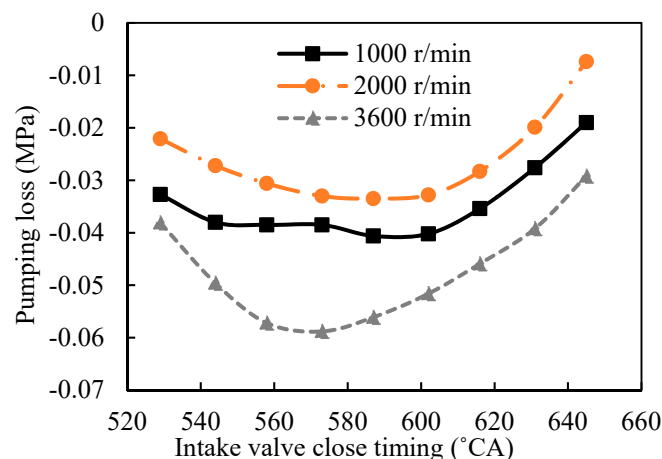

Figure 8. Effect of intake valve close timing on pumping loss at different speeds under 50% load.

Figure 7 shows that, as compared to the original engine, the throttle opening rose as Miller strength increased. Figures 7 and 8 demonstrate this point that the greater the Miller strength, the greater the throttle opening, and the smaller the pumping loss. This result is because the increased throttle opening reduced the intake throttle loss, which was beneficial to reduce the pumping loss. When the Miller strength reached 72 °CA, at 1000, 2000, and 3600 r/min, the pumping loss of the engine under 50% load was reduced by 51.1%, 77.6%, and 50.3% compared with the original engine, respectively. This part of the reduced pumping loss was one of the main reasons why the Miller cycle improved the engine fuel consumption under partial load operating conditions.

3.2. Influence of the Miller Cycle on the Cycle Efficiency under Partial Load Operating Conditions

In view of the change in pumping loss, 2000 r/min and 50% load were selected as the research conditions, and three schemes of Miller intensity, −44 °CA, 0 °CA, and 72 °CA, were selected to analyze the changes in the low pressure P-V diagram.

The comparison of low pressure P-V diagrams for three Miller cycle schemes under 50% load condition are shown in Figure 9. Because the throttle was not fully open, a certain vacuum degree was generated during the intake process of the piston downward, and a large loss of power was generated at that time. As a result of the increased throttle opening in the EIVC Miller cycle, the intake pressure was higher at that time than it was

in the original engine until the valve closed. With the downward movement of the piston producing a larger volume in-cylinder, the P-V diagram went through the process of pressure drop and rise. If the loss caused by heat transfer was not considered, this part of the pumping work changed was not significant. For the LIVC Miller cycle, also as a result of the increased throttle opening, the intake pressure at the early stage of intake was equivalent to EIVC, and both were higher than the original engine. However, as the piston moved down, the intake valve lift of the EIVC Miller cycle reached the maximum and the valve started to seat, while the intake valve of the LIVC Miller cycle still had a larger lift at that time. However, in the late intake valve closing scheme, after the valve was closed, the in-cylinder pressure curve in the compression process basically overlapped with the curve in the EIVC scheme. Considering that the three exhaust pressure curves basically overlap, the pumping loss was also mainly reflected in the change of the intake loss work.
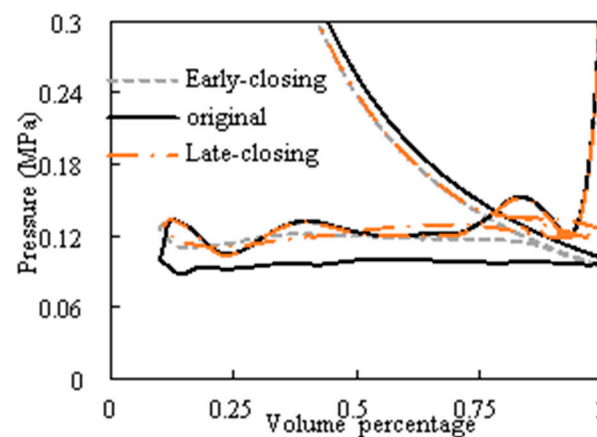

Figure 9. Comparison of low pressure P-V diagrams for three schemes.

The temperature and pressure in the combustion chamber were lower than in the original engine throughout the combustion process because the in-cylinder pressure and temperature were low at the initial moment of compression. The highest in-cylinder temperature was reduced by more than 10 K for both the EIVC and LIVC Miller cycles, as shown in Figure 10, for a comparison of the highest in-cylinder temperature at different intake valve closing times. Because of the decreased heat transfer, as illustrated in Figure 11, the Miller cycle was used after the cylinder heat transfer was reduced, resulting in an increase in useful work.
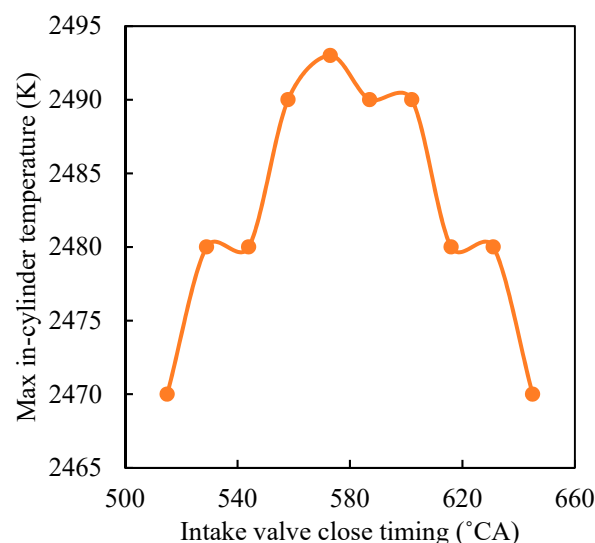

Figure 10. Effect of different intake valve close timing on maximum in-cylinder temperature.
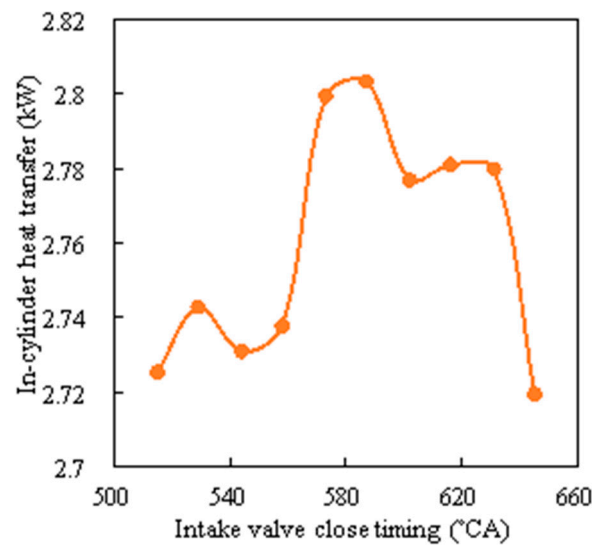
Figure 11. Effect of different intake valve close timing on in-cylinder heat transfer.

Therefore, it can be seen that the application of the Miller cycle under partial load operating conditions, due to the reduction of air intake volume, the throttle opening was increased compared with the original engine, so as to effectively reduce the pumping loss. At the same time, by decreasing the combustion temperature and maximum pressure in-cylinder while enhancing the cycle's thermal efficiency, cylinder heat transfer, knock, and NOx emissions may be minimized.

3.3. Effect of the Miller Cycle on the Fuel Economy under Full Load Operating Conditions

For the full load condition, simply using the approach of the early or late closing of the intake valve led to the decrease of the charging efficiency of the engine, which led to the reduction of the torque and could not meet the requirements of the engine dynamic performance. In order to maintain the same dynamic performance as the original engine, the intake pressure was changed by adjusting the nozzle diameter of the turbine in the turbocharger to ensure the same air intake volume, in order to study the influence of the Miller cycle on the engine performance under full load conditions.

Figure 12 shows the changes of the fuel consumption for the Miller cycle at different speeds under full load conditions. In general, for the EIVC of the Miller cycle, when the Miller intensity was greater than -29 °CA, the fuel consumption increased, because the intake valve closing time was too early and the intake valve lift and intake duration were too small. This was not conducive to the formation of the mixture in the cylinder, resulting in an increase in the fuel consumption. For the LIVC of the Miller cycle, the fuel consumption also first decreased and then increased. Because the intake valve closing time had too much delay, the effective compression ratio dropped significantly. This made the engine fuel consumption increase. For medium speeds, the application of the Miller cycle did not improve the engine fuel economy significantly, while for high speeds, the application of the Miller cycle with ELVC resulted in an increase in fuel consumption.

In this study, the turbocharger was used to improve the air intake volume; the efficiency of the turbocharger remained unchanged and the intake pressure was increased by reducing the nozzle diameter. Meanwhile, the improvement of the intake pressure inevitably is accompanied by an increase of exhaust pressure and exhaust resistance, which increases the pumping loss to a certain extent, especially the high-speed load, the pumping loss is more obvious. Figure 13 shows the influence of the closing time of the intake valve on the pumping loss under full load conditions at different speeds. It can be seen from the figure that as Miller intensity increases, the demand for intake pressure keeps increasing, and the pumping loss gradually increases. This part of the increased pumping loss offsets a part of

the effect brought by the Miller cycle. Therefore, to produce a more effective Miller cycle, the need for a high-efficiency turbocharger becomes particularly important.
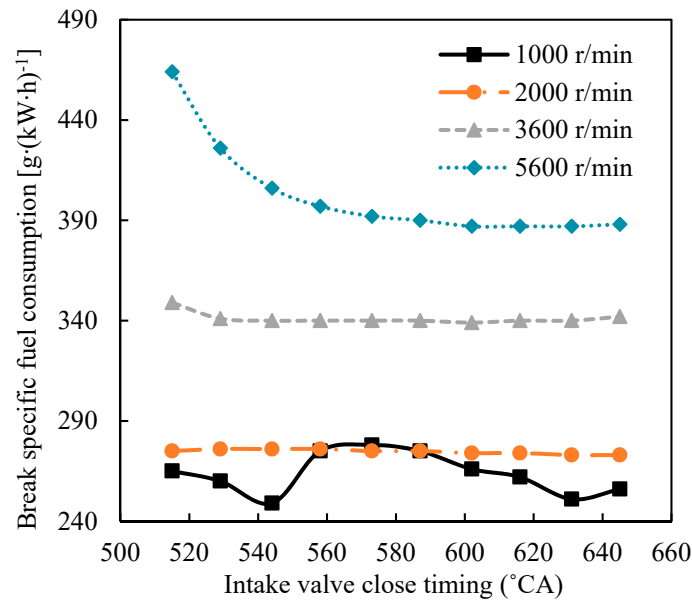

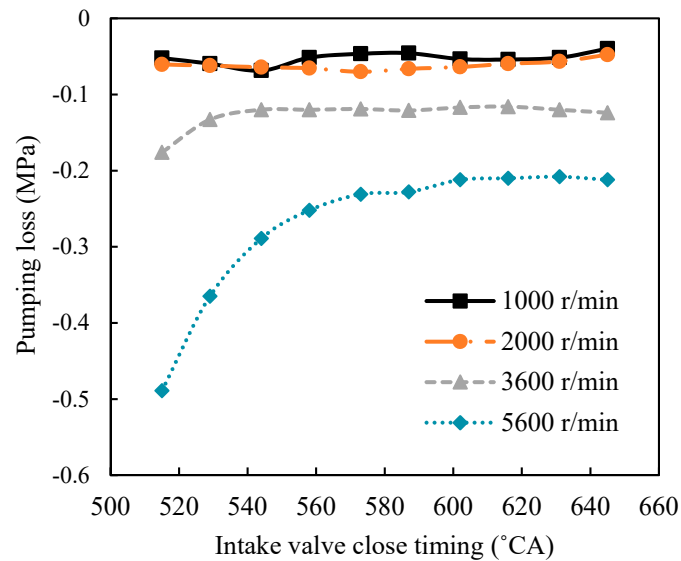**Figure 12.** Effect of the intake valve close timing on the fuel consumption at different speeds of under full load.

Figure 13. Effect of intake valve close time on pumping loss under different speeds of full load conditions.

3.4. Effect of EGR on the Engine with the Miller Cycle

Although EGR could reduce the in-cylinder combustion temperature, reduce nitrogen oxide emissions, and effectively suppress knocking, lower combustion temperatures would also reduce the combustion speed and maximum pressure in the cylinder, which is not conducive to improving the thermal efficiency of the engine. This section describes the study of the combination of the EGR system and the Miller cycle system to further improve engine fuel economy.

The 1D simulation model of EGR was built, an intake pipe and exhaust pipe based on the original model were added, and the abandoned EGR channel was added in the middle. One section was set as the forced cooling circuit, the EGR cooler was simulated, the whole

module was set, and the EGR valve opening was simulated through the flow coefficient of the regulator. The initial and boundary conditions of the simulation are shown in Table 4.

Table 4. Initial and boundary conditions of the simulation.

Project	Value
Initial intake temperature/K	336.2
Initial intake pressure/MPa	1.12
Initial temperature in-cylinder/K	820
Initial pressure in-cylinder/MPa	1.16
Cylinder head wall surface temperature/K	550
Cylinder wall surface temperature/K	450
Piston top temperature/K	450

Figure 14 shows the change of the EGR rate with the EGR valve flow coefficient (from 0.01 to 1) of the original machine, as well as the EIVC (515 °CA) and the LIVC (631 °CA) of the Miller cycle at a speed of 2000 r/min and 50% load. The EGR rate of the original machine was up to 21%, while the EIVC and LIVC were 12% and 13%, respectively. Because of partial loading of the original engine, the throttle opening was small and a certain negative pressure formed at the EGR outlet. After the Miller cycle was adopted, the throttle opening increased and the pressure at the EGR outlet increased, which caused the EGR flow resistance to increase. As a result, the EGR rate in the Miller cycle's LIVC was reduced, and the EGR rate in the Miller cycle's EIVC was the lowest. This was due to the fact that the EIVC of the Miller cycle had a lower charging efficiency than the LIVC of the Miller cycle under specific Miller intensities. As a result, the throttle opening of the Miller cycle's EIVC rose, the intake pressure increased, and the exhaust gas recirculation capacity reduced for the same intake flow rate.
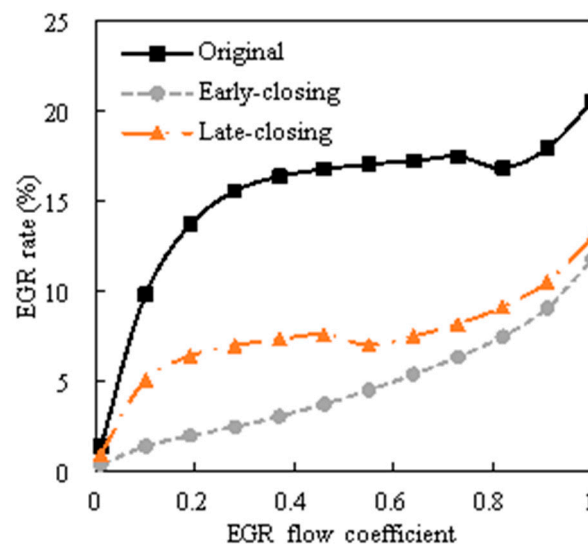

Figure 14. EGR rates for different flow coefficients of the EGR valve for the three schemes.

Figure 15 shows the influence of the EGR rate on fuel consumption rate for the original machine and the Miller cycle schemes of the EIVC and LIVC. The figure shows that the EGR rate was within 17%. The engine's fuel consumption could be continuously improved as the EGR rate increased. Furthermore, fuel consumption dropped by about 4.5 percent. When the EGR rate rose above 17%, as the EGR rate increased, the fuel economy deteriorated. This change was reflected in the EIVC and LIVC Miller cycles. For the LIVC Miller cycle, when the EGR rate was about 7%, the fuel consumption rate was the lowest, which was about 1.3% lower than the original engine at the same EGR rate, and about 3.2% lower than

that of the original engine without EGR. When the EGR rate was higher than 3%; however, the EIVC Miller cycle's fuel consumption deteriorated significantly.
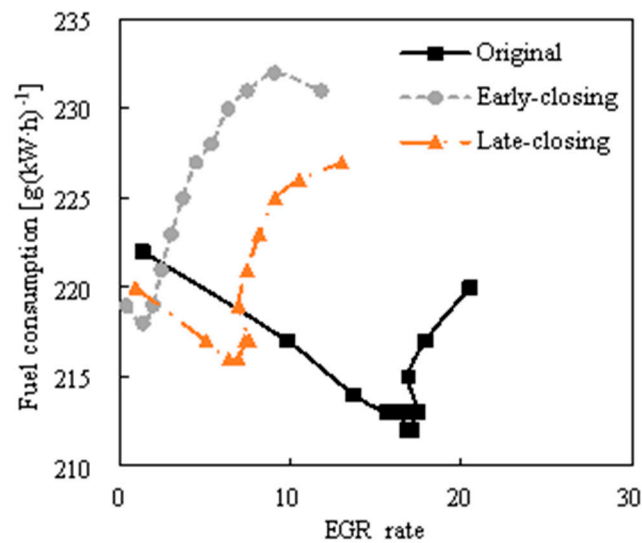

Figure 15. Effects of the EGR rate on the fuel consumption for the three schemes.

When the EGR system was applied to the engine, exhaust gas occupied part of the fresh air. To maintain the same dynamic characteristics as the original engine, it was necessary to increase the throttle opening and reduce the pumping loss. As shown in Figures 16 and 17, the EIVC and LIVC Miller cycle both increased with the EGR rate, gradually increasing the throttle opening, and gradually reducing the pumping loss, especially for the original engine. When the throttle opening was small, this improvement was more significant for the Miller cycle. When the throttle opening was large, the pumping loss was lower than that of the original engine.
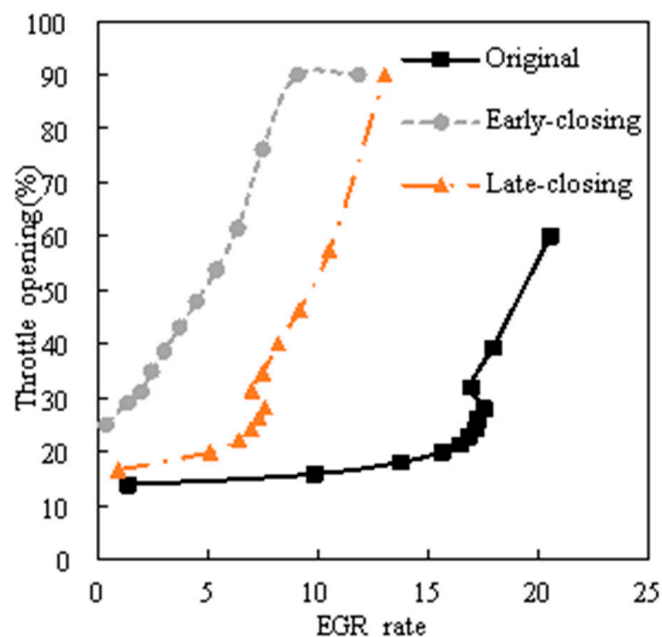

Figure 16. Effect of the EGR rate on the throttle opening for the three schemes.
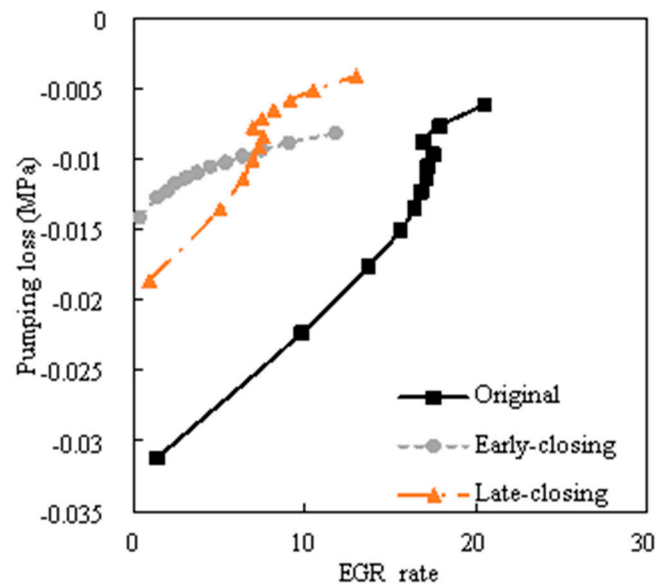
Figure 17. Effect of the EGR rate on the pumping loss for the three schemes.

Figure 18 shows that the maximum combustion temperature of in-cylinder gradually reduced as the EGR rate rose. The heat transported by the cylinder gradually reduced with the same heat transfer coefficient. This decrease in energy loss also resulted in a decrease in fuel usage.
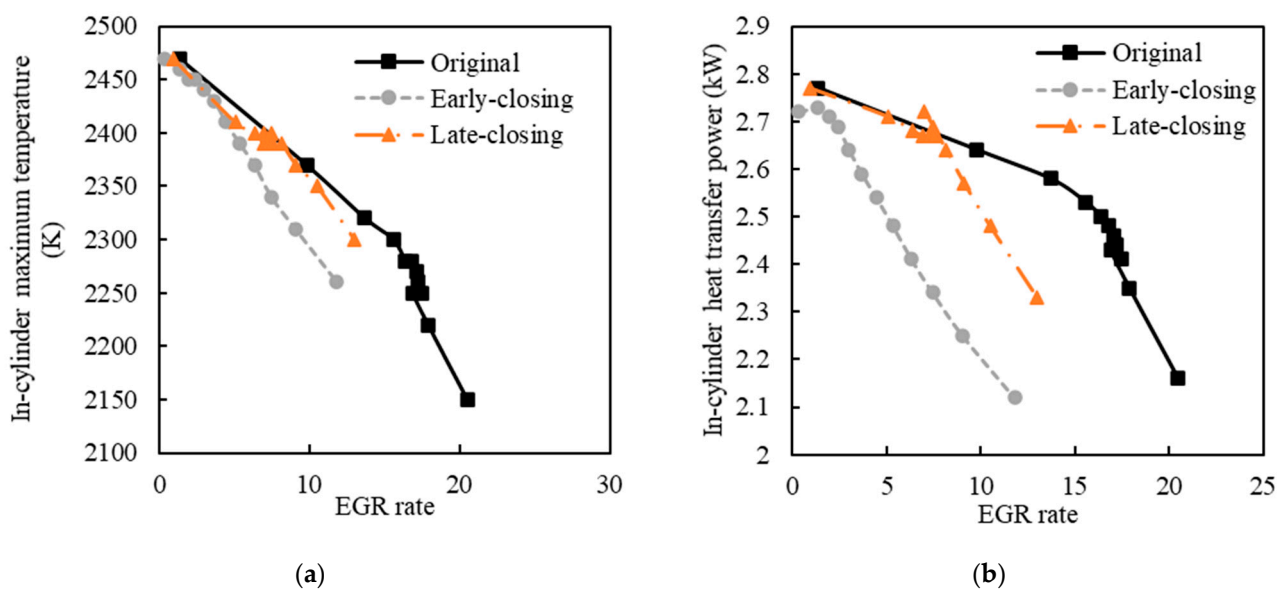

(**a**)　　　　　　　　　　　　　　　　　　　　　　　　　　　　　(**b**)

Figure 18. Effect of the EGR for the three schemes: (**a**) on the in-cylinder maximum temperature, (**b**) on the heat transfer power.

4. Conclusions

Based on a 1.5 T GDI engine, the influence of the Miller cycle and EGR on engine performance under partial load and full load situations were investigated using a calibrated 1D model in this study. The analysis led to the following conclusions:

(1)　At 50% load operating conditions, the Miller cycle could reduce fuel consumption by decreasing the pumping loss, increasing the intake density, and reducing the combustion temperature. Additionally, as the Miller intensity increased, the fuel consumption decreased. When the Miller intensity reached a maximum of 72 °CA, the

fuel consumption was lowered by 2.1%, 1.8%, and 2.4% at 1000, 2000, and 3600 r/min, respectively.

(2) At 1000 r/min and full load operating conditions, the Miller cycle had a significant effect on increasing the engine's fuel efficiency. In the LIVC Miller cycle, the decrease in fuel consumption reached a maximum of 9.7% when the Miller intensity was 58 °CA, and the fuel consumption decreased by 10.5% when the EIVC Miller intensity was −29 °CA.

(3) At 2000 r/min and 50% load operating conditions, EGR was combined with the Miller cycle. When the EGR rate rose on the original engine, the fuel consumption first dropped and then improved, and the fuel consumption decreased by at least 4.5%. The best fuel consumption rate was in the LIVC Miller cycle, when the EGR rate was around 7%. Furthermore, the fuel consumption was reduced by about 1.3% compared with the original engine at the same EGR rate, and the fuel consumption was about 3.2% lower than that of the original engine without EGR.

The potential of the Miller cycle paired with EGR technology in boosting engine fuel efficiency has been demonstrated through numerical simulation analyses in this paper. Future research will combine this technology with the combustion process and durability of the engine to achieve fuel economy improvement.

Author Contributions: S.W., methodology, investigation, writing—original draft, and project administration; Z.Z., conceptualization, writing—review and editing, and software; X.L., software and data curation; C.W., investigation and visualization; F.Y., software and investigation. All authors have read and agreed to the published version of the manuscript.

Institutional Review Board Statement: Not applicable.

Informed Consent Statement: Not applicable.

Data Availability Statement: Some data, models, or code that support the findings of this study are available from the corresponding author upon reasonable request.

Conflicts of Interest: The authors declare no conflict of interest.

References

1. Hunicz, J.; Mikulski, M.; Koszałka, G.; Ignaciuk, P. Detailed analysis of combustion stability in a spark-assisted compression ignition engine under nearly stoichiometric and heavy EGR conditions. *Appl. Energy* **2020**, *280*, 115955. [CrossRef]
2. Wróblewski, P.; Koszalka, G. An Experimental Study on Frictional Losses of Coated Piston Rings with Symmetric and Asymmetric Geometry. *SAE Int. J. Engines* **2021**, *14*, 853–866. [CrossRef]
3. Wróblewski, P.; Iskra, A. *Problems of Reducing Friction Losses of a Piston-Ring-Cylinder Configuration in a Combustion Piston Engine with an Increased Isochoric Pressure Gain*; SAE Technical Paper 2020-01-2227; SAE Tech: Shanghai, China, 2020.
4. Huang, Z.; Shen, K.; An, Z.; Chen, W.; Pan, J. Effects of Miller Cycle of Different Compression Ratios and Low Pressure EGR on Performance of Turbocharged Gasoline Direct Injection Engine. *Chin. Intern. Combust. Engine Eng.* **2019**, *40*, 13–18.
5. Martins, M.; Lanzanova, T. Full-load Miller cycle with ethanol and EGR: Potential benefits and challenges. *Appl. Therm. Eng.* **2015**, *90*, 274–285. [CrossRef]
6. Neyestani, S.E.; Walters, S.; Pfister, G.; Kooperman, G.J.; Saleh, R. Direct Radiative Effect and Public Health Implications of Aerosol Emissions Associated with Shifting to Gasoline Direct-Injection (GDI) Technologies in Light-duty Vehicles in the United States. *Envrion. Sci. Technol.* **2020**, *54*, 687–696. [CrossRef]
7. Ji, W.; Li, A.; Lu, X.; Huang, Z.; Zhu, L. Numerical study on NOx and ISFC co-optimization for a low-speed two-stroke engine via Miller cycle, EGR, intake air humidification, and injection strategy implementation. *Appl. Therm. Eng.* **2019**, *153*, 398–408. [CrossRef]
8. Iodice, P.; Giuseppe, L.; Amoresano, A. Ethanol in gasoline fuel blends: Effect on fuel consumption and engine out emissions of SI engines in cold operating conditions. *Appl. Therm. Eng.* **2018**, *130*, 1081–1089. [CrossRef]
9. Miklanek, L.; Vitek, O.; Gotfryd, O.; Klir, V. Study of unconventional cycles (Atkinson and Miller) with mixture heating as a means for the fuel economy improvement of a throttled SI engine at part load. *SAE Int. J. Engine* **2012**, *5*, 1624–1636. [CrossRef]

10. Patel, R.; Ladommatos, N.; Stansfield, P.A.; Wigley, G.; Garner, C.P.; Pitcher, G.; Turner, J.W.; Nuglisch, H.; Helie, J. Unthrottling a direct injection gasoline homogeneous mixture engine with variable valve actuation. *Int. J. Engine Res.* **2010**, *11*, 391–411. [CrossRef]

11. Gonca, G. Comparative performance analyses of irreversible OMCE (Otto Miller cycle engine)-DiMCE (Diesel miller cycle engine)-DMCE (Dual Miller cycle engine). *Energy* **2016**, *109*, 152–159. [CrossRef]

12. Chen, B.; Zhang, L.; Han, J.; Zhang, Q. A combination of electric supercharger and Miller Cycle in a gasoline engine to improve thermal efficiency without performance degradation. *Case Stud. Therm. Eng.* **2019**, *14*, 100429. [CrossRef]

13. Alasdair, C.; Hugh, B.; Graham, I. *Exhaust Gas Recirculation for Improved Part and Full Load Fuel Economy in a Turbocharged Gasoline Engine*; SAE Technical Paper 2006-01-0047; SAE Tech: Shanghai, China, 2006.

14. Rakopoulos, D.C.; Rakopoulos, C.D.; Kosmadakis, G.M.; Giakoumis, E.G. Exergy assessment of combustion and EGR and load effects in DI diesel engine using comprehensive two-zone modeling. *Energy* **2020**, *202*, 117685. [CrossRef]

15. Yin, T.; Li, T.; Zhen, B.; Zhao, F. Optimization of Fuel Economy for Turbocharged Gasoline Engine Based on Cooled EGR and Compression Ratio. *Veh. Engine* **2016**, *2*, 28–34.

16. Li, J.; Yu, X.; Xie, J.; Yang, W. Mitigation of high pressure rise rate by varying IVC timing and EGR rate in an RCCI engine with high premixed fuel ratio. *Energy* **2020**, *192*, 116659. [CrossRef]

17. Su, J.; Xu, M.; Li, T.; Yi, G.; Wang, J. Combined effects of cooled EGR and a higher geometric compression ratio on thermal efficiency improvement of a downsized boosted spark-ignition direct-injection engine. *Energy Convers. Manag.* **2014**, *78*, 65–73. [CrossRef]

18. Zhao, J. Research and application of over-expansion cycle (Atkinson and Miller) engines-A review. *Appl. Energy* **2017**, *185*, 300–319. [CrossRef]

19. Li, T.; Gao, Y.; Wang, J.; Chen, Z. The Miller cycle effects on improvement of fuel economy in a highly boosted, high compression ratio, direct-injection gasoline engine: EIVC vs. LIVC. *Energy Convers. Manag.* **2014**, *79*, 59–65. [CrossRef]

20. Cleary, D.; Silvas, G. *Unthrottled Engine Operation with Variable Intake Valve Lift, Duration, and Timing*; SAE Technical Paper 2007-01-1282; SAE Tech: Shanghai, China, 2007.

21. Wan, Y.; Du, A. *Reducing Part Load Pumping Loss and Improving Thermal Efficiency through High Compression Ratio Over-Expanded Cycle*; SAETechnical Paper 2013-01-1744; SAE Tech: Shanghai, China, 2013.

22. He, Y.; Liu, J.; Zhu, B.; Sun, D. Development of a Miller cycle engine with single-stage boosting and cooled external exhaust gas recirculation. *Proc. Inst. Mech. Eng. Part D J. Automob. Eng.* **2017**, *231*, 766–780. [CrossRef]

23. Alger, T.; Gingrich, J.; Roberts, C.; Mangold, B. Cooled exhaust-gas recirculation for fuel economy and emissions improvement in gasoline engines. *Int. J. Engine Res.* **2011**, *12*, 252–264. [CrossRef]

24. Fontana, G.; Galloni, E. Experimental analysis of a spark-ignition engine using exhaust gas recycle at WOT operation. *Appl. Energy* **2010**, *87*, 2187–2193. [CrossRef]

25. Zhang, Z.; Zhang, H.; Wang, T.; Jia, M. Effects of tumble combined with EGR (exhaust gas recirculation) on the combustion and emissions in a spark ignition engine at part loads. *Energy* **2014**, *65*, 18–24. [CrossRef]

26. Liu, Z.; Cleary, D. *Fuel Consumption Evaluation of Cooled External EGR for a Downsized Boosted SIDI DICP Engine*; SAE Technical Paper 2014-01-1235; SAE Tech: Shanghai, China, 2014.

27. Song, D.; Jia, N.; Guo, X.; Ma, X.; Ma, Z.; Gao, D.; Li, K.; Lai, H.; Zhang, C. *Low Pressure Cooled EGR for Improved Fuel Economy on a Turbocharged PFI Gasoline Engine*; SAE Technical Paper 2014-01-1240; SAE Tech: Shanghai, China, 2014.

28. Wang, J.; Xu, M.; Su, J.; Gao, Y. Influences of Engine LIVC on Fuel Economy and Soot Emission. *Veh. Engine* **2014**, *3*, 21–24.

29. Yang, X.; Liao, C.; Liu, J. Harmonic analysis and optimization of the intake system of a gasoline engine using GT-power. *Energy Procedia* **2012**, *14*, 756–762. [CrossRef]

30. Trajkovic, S.; Tunestål, P.; Johansson, B. *Simulation of a Pneumatic Hybrid Powertrain with VVT in GT-Power and Comparison with Experimental Data*; SAE Technical Paper 2009-01-1323; SAE Tech: Shanghai, China, 2009.

31. Sun, Y.; Zhu, Z.; Du, A.; Chen, X. Multiparameter Optimization Framework of Cyberphysical Systems: A Case Study on Energy Saving of the Automotive Engine. *Actuators* **2021**, *10*, 330. [CrossRef]